

PIEZOELECTRIC ACTUATOR ARRAY FOR MOTION-ENABLED RECONFIGURABLE RF CIRCUITS

Mary C. Tellers^{1,2}, Jeffrey S. Pulskamp¹, Sarah S. Bedair¹,

Ryan Q. Rudy¹, Iain M. Kierzewski¹, Ronald G. Polcawich¹ and Sarah E. Bergbreiter²

¹Sensors and Electron Devices Directorate, Army Research Laboratory, Adelphi, MD, USA

²Mechanical Engineering, University of Maryland, College Park, College Park, MD, USA

ABSTRACT

This paper reports on the translation and rotation capabilities of arrays of piezoelectrically actuated MEMS cantilevers developed for a motion-enabled reconfigurable radio frequency (RF) circuit micro-factory, known as RFactory. The reported actuator surface demonstrates 2.4 to 100 times faster translational speeds than similar devices, depending on the actuation technology used for comparison. The array was driven with different waveforms, voltages, and frequencies to characterize the quality of motion of a silicon chip placed on the array. It has demonstrated instantaneous velocities of 20 mm/s, maximum average velocities of 3.5 mm/s, and rotational speeds of 31.9 rpm at sub-10 V actuation and less than 2% off-axis translational deviation. The effort has identified significant operational and design variables using the first dynamic contact model developed for micromanipulation surfaces.

KEYWORDS

Micromanipulation, piezoelectric actuators, reconfigurable circuits, MEMS conveyance.

BACKGROUND

RFactory is an effort to create motion-enabled reconfigurable circuits that avoid transmission line losses and design tradeoffs that switch matrix approaches to circuit reconfiguration face. The intended applications of RFactory are consistent with the goals of the DARPA RF Field Programmable Gate Array “RF-FPGA” program [1].

Figure 1 illustrates the motion-enabled circuit reconfiguration concept. The RFactory consists of a MEMS actuator surface that positions and orients die-level or packaged RF circuit components, such as filters and amplifiers, beneath an interconnect substrate. This substrate features an array of mechanically compliant contacts and transmission lines that permits chips to be electrically connected once a bulk piezoelectric actuator presses them vertically into contact. This approach ultimately allows the position and orientation of individual electronic components to determine the circuit configuration. Precision and repeatability in the actuator surface will lead to reduced contact resistance variation, more flexibility in component size selection, and overall electronic performance.

Actuator Surface

The problem of precisely conveying micro-scale parts has been addressed through a variety of approaches.

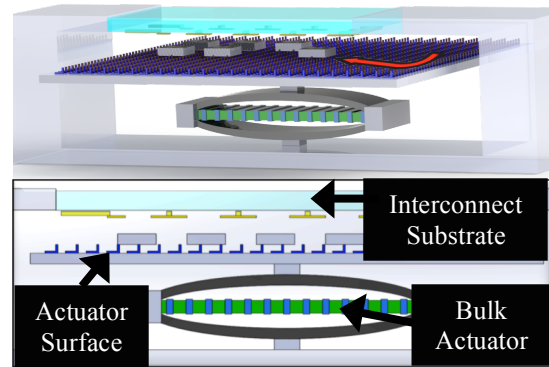


Figure 1: Illustration of the RFactory system. Electronic components on the actuator surface are connected via the interconnect substrate once raised by the bulk actuator.

Micromanipulation surfaces using electro-thermal, electrostatic, and air-flow actuation have been investigated for years. Work on active surfaces with MEMS thermal bimorphs showed maximum speeds of 1 mm/s and rotational speeds of 1.7 rpm [2]. Electrostatic MEMS devices developed for parts-sorting applications have demonstrated maximum speeds of 0.2 mm/s [3]. MEMS-based actuator arrays for air-flow distributed micromanipulation were shown to be capable of 8.3 mm/s linear translation, although they are not compatible with millimeter-scale objects [4]. These technologies have demonstrated translation and rotation of parts using MEMS.

The unit actuator employed in this work is shown in Figure 2. The device is a unimorph d_{31} -mode piezoelectric cantilever actuator fabricated through a thin-film PZT and multi-layer-metal process developed previously by Bedair et al. [5]. The application of voltage to the parallel plate electrodes induces out-of-plane bending. High aspect ratio metal posts at the free end amplify the actuator deflections in the desired direction of motion. A component in contact with the posts acquires the actuator velocity in the absence of contact slip and transitions to projectile motion with sufficient chip velocity and actuator deceleration. These small “hops” toward the anchored side of the actuator are on the order of microns per step. Reasonable chip velocities can be attained by repeating these motions at high frequency. Orthogonally arrayed sets of actuators can induce bi-directional motion. Rotation is achieved by utilizing sets of arrays of the same unit actuators, in opposite directions, to apply force couples (Figure 3B).

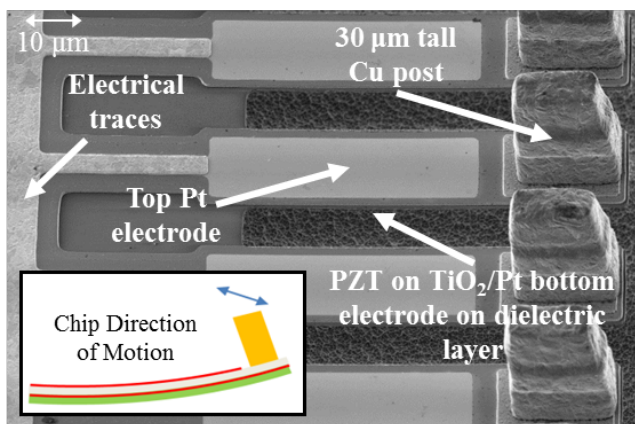


Figure 2: SEM of RFactory actuator surface array. The illustration inset shows how the tall metal posts enhance motion in the horizontal direction.

MODEL DEVELOPMENT

Two models were developed to provide insight into the operation of the actuator surface devices. A simple quasi-static model of piezoelectric actuation and a detailed dynamic model incorporating the influence of higher order vibrational modes were developed to most completely describe component motion on the actuator surface. The quasi-static model obtains the vertical and lateral displacements at the top of the posts and calculates velocities based on the frequency of operation and basic waveform parameters. The dynamic model expanded upon previous work developed to describe the dynamics of micro-switches [6]. The model relies on modal decomposition to include the effects of higher-order vibrational modes. Finite element analysis is used to obtain modal parameters, such as resonant frequencies and mode shapes, and the resulting modal forces and time domain dynamics are obtained analytically. The actuator surface model was expanded to include contact dynamics such as modal transitions (modes associated with and without chip contact), friction, and friction-modulated adhesion. Both models utilize nonlinear piezoelectric material properties (e.g. electric field dependent piezoelectric coefficients).

EXPERIMENTAL EVALUATION

Experimental Set-up

The experimental results consist of two phases: initial testing and more detailed characterization work. Initially, +X, +/-X, +/-XY, and rotational arrays were tested to demonstrate the flexibility in designs possible with these cantilevers, examples of which are seen in Figure 3.

The characterization results presented are from one device with $90\ \mu\text{m} \times 16\ \mu\text{m}$ actuator electrodes and $20\ \mu\text{m}$ tall gold posts. Each data point represents averaged values from three tests composed of 300-1500 frames of video. The error bars represent one standard deviation. Numerous devices have been characterized; the results presented are

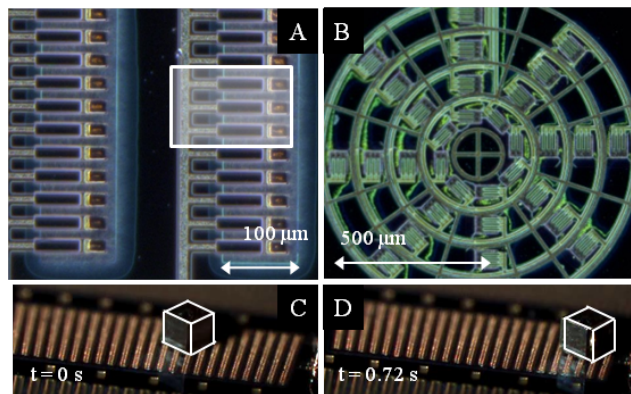


Figure 3: A) Optical image of actuator array. Highlighted area is what is imaged in Figure 1. B) Rotational actuator array layout. C & D) Time sequence using highlighted silicon chip ($500\ \mu\text{m}$ cube) to show conveyance of a "component" across the array.

generally representative of performance.

Using a Keyence high-speed microscope, the motion of a $500\ \mu\text{m} \times 500\ \mu\text{m} \times 500\ \mu\text{m}$ silicon chip on the actuator surface was recorded as the actuation signal was applied. Keyence Motion Analyzer software obtained the position and orientation of the chip during the test.

The metrics of note were velocity in the intended direction of motion (called X velocity), and distance interval error jitter (DIE jitter), which is used to characterize the irregularity of the motion. DIE jitter is analogous to timing interval error in precision oscillators [6]. It is used in cases where the chip velocity is anticipated to be uniform. The DIE jitter is normalized to translational and rotational error such that a value equal to or less than one means less than $100\ \mu\text{m}$ on-axis (X) error, $200\ \mu\text{m}$ off-axis (Y) error, and 10° rotational displacement when extrapolated to 5 mm of translation. X velocity and DIE jitter sufficiently characterize the speed and precision of the actuator surface despite the complex behavior exhibited by the system over frequency, voltage amplitude, and waveform parameters.

Three parameters were investigated for controlling chip motion: voltage amplitude, frequency, and waveform parameters. Voltage amplitude tests reveal the critical voltage necessary for translation for a device design. Experiments varying excitation frequency show that device behavior is highly sensitive to the frequency of operation. Several waveforms were initially tested, such as square, sine, and ramp waves. Ramp waves were shown to have the best trade-off between speed and jitter. Further waveform testing examined the impact of symmetry of ramp waves on operation. Despite the overall complexity of the device response, certain operating conditions have been identified that provide desirable and repeatable chip motion, such that the translational error is $300\ \mu\text{m}$ with a standard deviation of $145\ \mu\text{m}$ and a rotational error of 8° with a standard deviation of 4.8° for an extrapolated translation of 5 mm.

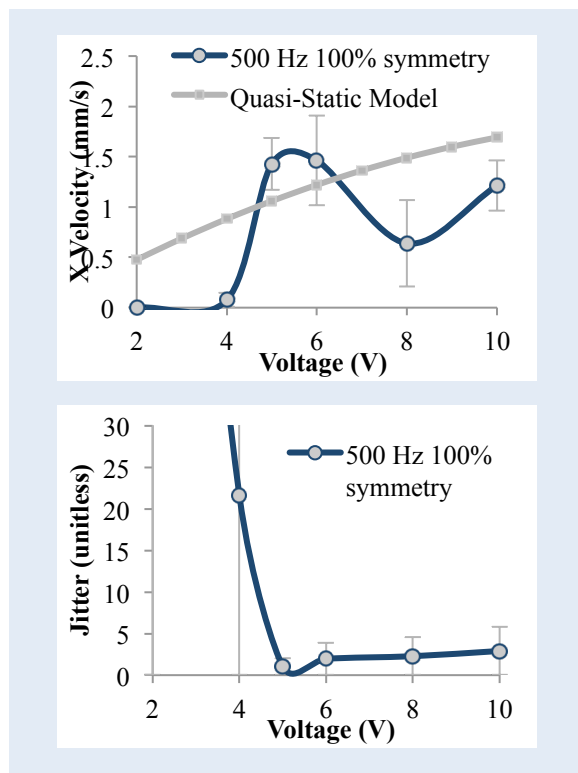


Figure 4: Top: The experimental results show that contrary to the quasi-static model, low voltage amplitudes are not capable of significant translation. Bottom: Above 4 V, the jitter gradually rises. At low voltage amplitudes, jitter is high due to a lack of translation.

Experimental Results

Initial testing of +X, +/-X, and rotational stages demonstrated performance consistent with the basic requirements of the RFactory system. Speeds as high as 20 mm/s were observed, with a maximum average velocity of 3.5 mm/s. The average translational speeds are three times higher than previous results with thermal bimorphs [1] and 17.5 times faster than electrostatic actuators [2]. Rotational speeds of 31.9 rpm were achieved with the rotational stage seen in Figure 3B. The RFactory actuator surface rotational speed is nearly thirty times faster than thermal bimorphs [1].

Amplitude testing from 2 V to 10 V revealed preferential regions of operation, with good velocities above 4 V (see Figure 4). The quasi-static model predicts that X velocity will increase with voltage amplitude, but the experimental results show some deviation from this trend. The corresponding DIE jitter shows that operation above 4 V is advantageous for speed as well as precision. Above 5 V, however, the jitter gradually rises. At low voltages, the deflection is insufficient for significant motion, leading to rapid bi-directional rotation and thus high jitter levels.

In general, increased frequency leads to increased velocity, as the total motion is essentially a summation of the “hop” displacements caused by each cycle of actuation, as seen in the quasi-static model in Figure 5. Figure 6 illustrates the agreement between the dynamic model and

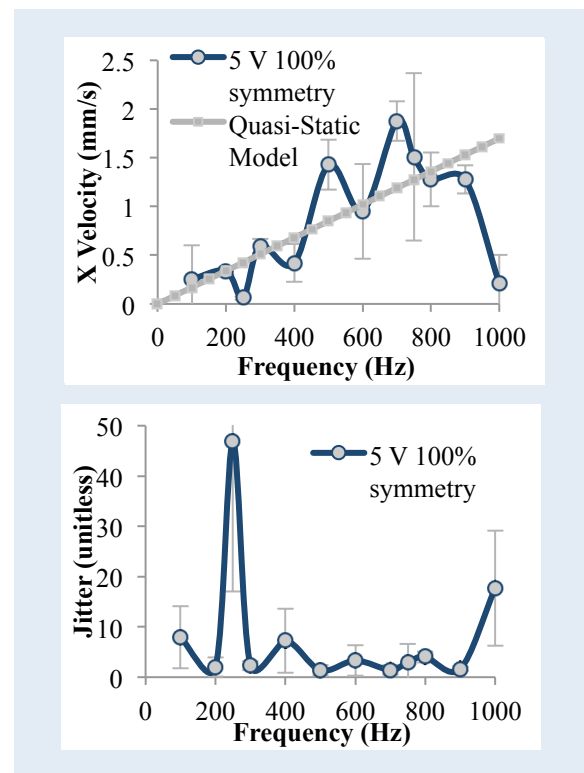


Figure 5: Top: The X velocity response to frequency generally follows the quasi-static model until 800 Hz. Bottom: Jitter levels show good operation at 300-800 Hz.

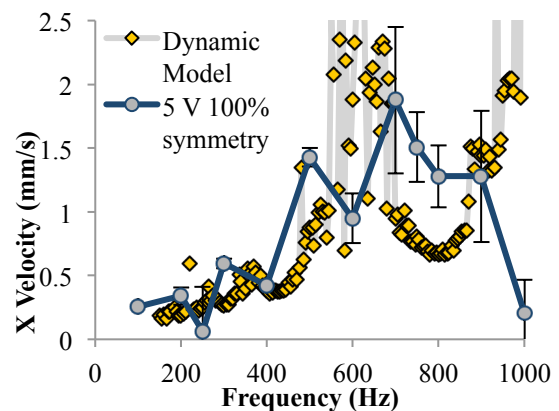


Figure 6: The dynamic model and the experimental results agree qualitatively. The model and experimental data agree most closely at low frequencies, where the higher-order vibrational modes play a smaller role.

the experimental values. The largest discrepancies are seen in areas where the model is unstable, likely due to higher-order vibrational modes. The strong qualitative agreement between the dynamic model and the experimental results indicates that many of the contributing parameters, like adhesion and contact transition behavior, influence the deviation from the quasi-static model seen in Figure 5. By operating the actuator surface at the peak velocity values in the low-jitter region of 500 to 700 Hz, rapid and precise conveyance can be achieved. For example, 700 Hz

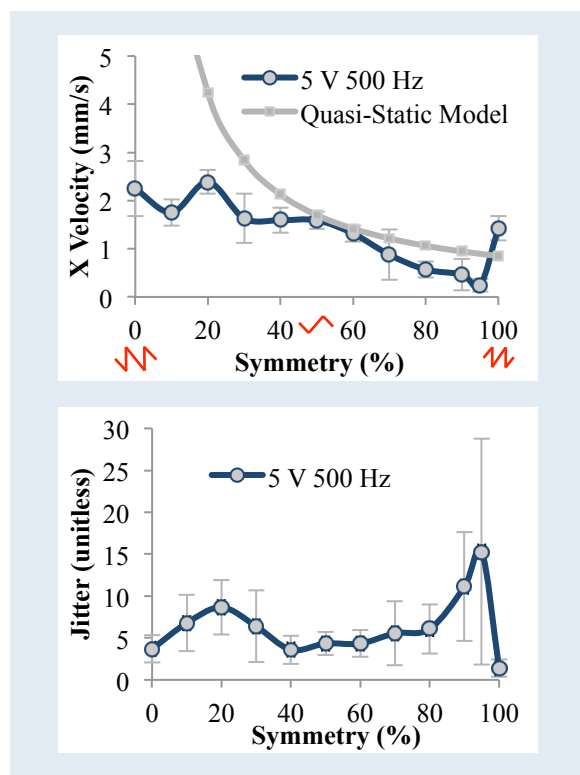


Figure 7: Top: Symmetry can strongly impact velocity. Waveforms at 0%, 50% and 100% symmetry inset. Bottom: 100% symmetry has the lowest jitter level, with other low values between 40% and 80%.

operating frequency leads to almost 2 mm/s average velocity and sub-2 jitter levels. Frequency is one of the most sensitive and important parameters to control for good motion quality.

Using the ramp waveform, a range of symmetries was investigated. Symmetries from 0% to 100% were tested at 5 V and 500 Hz. Symmetry determines the percent of the period that is used to ramp the signal from 0 V to the peak voltage, i.e. at 0% symmetry, the signal is a step-up, ramp down signal. X Velocity and jitter results seen in Figure 7 show the most preferential behavior at 100% symmetry and between 40% and 80%. The quasi-static model is least accurate in predicting symmetry response, especially because low symmetry at a given voltage and frequency will increase peak actuator accelerations, which leads to complex dynamics not accounted for in the quasi-static model.

CONCLUSIONS

A piezoelectric MEMS actuator surface capable of conveying discrete circuit components has been designed, fabricated, modeled, and characterized. A dynamic model, extended from MEMS contact switch modeling, was applied for the first time to a contact-based micro-manipulation device. This model matches well qualitatively with the complex experimental response of the system. Voltage amplitude, frequency, and ramp wave symmetry were

investigated to control speed and precision of motion. For low jitter and good velocity, initial results suggest operating voltages from 4 to 10 V with operating frequencies in the 500-700 Hz range using a 100% symmetry ramp wave.

This work led to a more complete understanding of the complex dynamics of actuation and the utility of voltage amplitude, frequency, and symmetry to manipulate motion quality. Future work aims to characterize the impact of design parameters, such as length and width of actuators, on component motion. The actuator surface will be refined through design and appropriate operation to obtain the speed and precision required for the RFactory effort. Additional efforts to integrate capacitive sensing to enable closed-loop control of the actuator surface will also be addressed.

ACKNOWLEDGEMENTS

The authors would like to acknowledge DARPA/MTO for financial support. Additionally, the authors would like to acknowledge Luz Sanchez, Brian Power, Joel Martin, and Steven Isaacson for assistance in fabricating devices.

REFERENCES

- [1] M. Lee, M. Lucas, R. Young, R. Howell, P. Borodulin, and N. El-Hinnawy, "RF FPGA for 0.4 to 18 GHz DoD Multi-function Systems," GOMACTech-13, Las Vegas, NV, (2013), pp. 111-114.
- [2] J. W. Suh, R. B. Darling, K.-F. Bohringer, B. R. Donald. "CMOS integrated ciliary actuator array as a general-purpose micromanipulation tool for small objects," Journal of Microelectromechanical Systems, 8, (1999).
- [3] K.-F. Bohringer, J. W. Suh, B. R. Donald, and G. T. A. Kovacs. "Vector fields for task-level distributed manipulation: experiments with organic micro actuator arrays," Proceedings of the 1997 International Conference on Robotics and Automation, Albuquerque, NM, (1997), pp. 1779-1786.
- [4] Y. Fukuta, Y.-A. Chapuis, Y. Mita, and H. Fujita. "Design, fabrication, and control of MEMS-based actuator arrays for air-flow distributed micromanipulation." Journal of Microelectromechanical Systems, 15, (2006).
- [5] S. S. Bedair, J.S. Pulskamp, C. D. Meyer, R. G. Polcawich, and I. M. Kierzewski. "Modeling, fabrication and testing of MEMS tunable inductors varied with piezoelectric actuators," Journal of Micromechanics and Microengineering, 24, 095017, (2014).
- [6] J. S. Pulskamp, R. M. Proie, Jr., R. G. Polcawich. "Nano- and micro-electromechanical switch dynamics," Journal of Micromechanics and Microengineering, (2013).
- [7] National Instruments, "Understanding and Characterizing Timing Jitter", 2013.

CONTACT

*Jeffrey S. Pulskamp, tel +1-301-394-0016;
jeffrey.s.pulskamp.civ@mail.mil